ELSEVIER

Polymer 43 (2002) 1483–1490

polymer

www.elsevier.com/locate/polymer

Ultrasonic absorption and relaxations in ABS composite polymers

Kazuhito Nishikawa[a,1], Yuji Hirose[a], Osamu Urakawa[a], Keiichiro Adachi[a,*], Akira Hatano[b], Yuji Aoki[b]

[a]*Department of Macromolecular Science, Graduate School of Science, Osaka University, 1-1 Machikaneyama-cho, Toyonaka, Osaka 560-0043, Japan*
[b]*Yokkaichi Research Center, Mitsubishi Chemical Corporation, 1 Toho-cho, Yokkaichi 510-8530, Japan*

Received 23 March 2001; received in revised form 1 July 2001; accepted 9 August 2001

Abstract

We investigated ultrasonic attenuation, dynamic Young's modulus, Izod impact strength, and dielectric relaxation of acrylonitrile–butadiene–styrene composite polymers (ABS) in which styrene-co-butadiene rubber particles are dispersed in styrene-co-acrylonitrile random copolymer. High ultrasonic attenuation was observed around 240 K and the intensity of attenuation increased with increasing rubber content. Temperature dependence curves of dielectric loss in the frequency range from 12 Hz to 200 kHz and temperature range from 80 to 420 K exhibited four relaxation processes designated as the α, β′, β, and γ. From the relaxation map produced for the mechanical and dielectric relaxations, the ultrasonic absorption was attributed to the β and β′ processes. It was deduced that inter-grain thermoelastic process, also contribute to the ultrasonic attenuation. Correlation was found between the ultrasonic absorption and the Izod impact strength indicating that the high impact strength of ABS is partly due to the effective absorption of impact energy through those relaxation processes.

Keywords: Acrylonitrile–butadiene–styrene composite polymers; Ultrasonic attenuation; Dielectric relaxation

1. Introduction

Acrylonitrile–butadiene–styrene (ABS) composite polymer is an impact-resistant polymer and used widely in industry [1,2]. In this polymer, rubber particles of polybutadiene or styrene-co-butadiene random copolymer (SBR) are dispersed in glassy styrene-co-acrylonitrile random copolymer (SAN). The SAN molecules are grafted at the surface of the rubber particles. Similar structure and mechanical properties are known for high impact strength polystyrene (HIPS) [2–4]. Matsuoka [5] investigated the effects of various factors on the Izod impact strength of polymers and found the brittle to ductile transition temperature where the behaviour of fracture changes. Brittle fracture of glassy polymers by a mechanical impact occurs through the formation of crazes or cracks and subsequent growth of them. So far many studies of high impact resistant polymers were made to understand the mechanisms of impact strength of polymers and the importance of the surface energy to create cracks was pointed out [6–8]. Andrews and Reed reviewed the theories and experimental studies of fracture of polymers focusing their attention to the relationship between the surface energy and rupture of chemical bonds [6]. For ABS the mechanical properties in relation to the impact strength were reported by several authors [9–12]. For ABS or HIPS it is also believed that the high impact strength is due to stop of growth of cracks at the surface of the rubber particles [9].

Besides those mechanisms of formation and growth of cracks, dissipation of impact energy which effectively prevents formation and growth of cracks is an important factor of high impact strength of polymers. A mechanical impact can be regarded as a shock wave and is generally represented by the sum of its Fourier components. Therefore, an impact is composed of sound waves of various frequencies. When the duration of a spike is very short, its Fourier components distribute over a wide frequency range. Those sound waves are attenuated and the impact energy is dissipated into thermal energy. If the impact energy is attenuated quickly, crazes or cracks are not formed and even if they were formed, they would not grow much. From this point of view, we expect that there is a relationship between the attenuation of ultrasonic sound waves and the high impact strength of ABS.

Since the sound velocity and attenuation are related,

* Corresponding author. Tel./fax: +81-66-850-5464.
E-mail address: adachi@chem.sci.osaka-u.ac.jp (K. Adachi).
[1] Address: Sumitomo Rubber Industry, 4-1 Shinsei-cho, Toyota, 471-0837, Japan.

0032-3861/02/$ - see front matter
PII: S0032-3861(01)00664-4

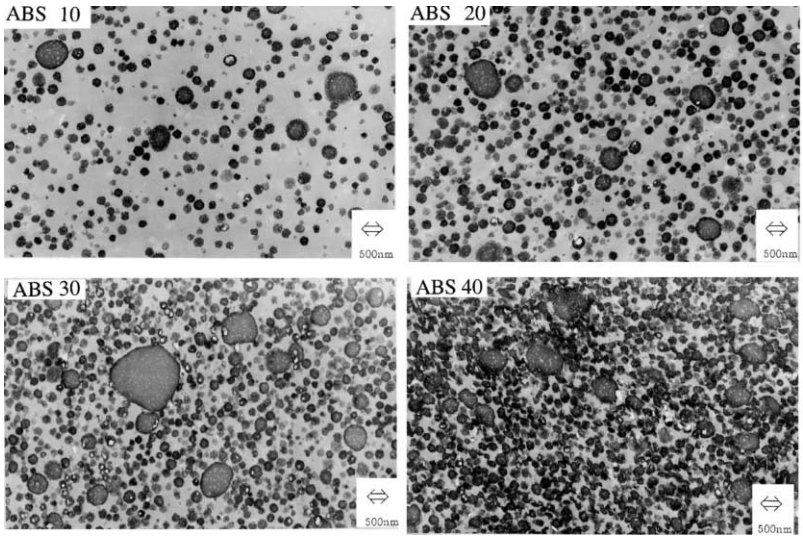

Fig. 1. Transmission electron micrographs of ABS samples. The dark regions are due to the rubber phase.

respectively, to the storage and loss moduli at the frequency of the sound [13], the ultrasonic attenuation can be understood primarily as a high frequency loss modulus due to Brownian motions of polymer segments. However, there are additional mechanisms of the attenuation which are characteristic of the ultrasound propagation such as thermoelastic absorption, scattering, and phonon–phonon interactions [14–16]. Especially in heterogeneous systems, the mechanism called inter-grain thermoelastic effect cannot be neglected [17,18]. These processes cannot be detected by the other methods such as dielectric and low frequency mechanical relaxation. We can distinguish the ultrasonic attenuation due to the segmental motions from these latter processes by comparison of the ultrasonic and dielectric relaxation. Yeow et al. reported the dielectric relaxation behaviour of ABS [19]. They found that there exist seven relaxation processes. In this paper, we re-examine the dielectric and mechanical relaxation behaviour of ABS. The objective of the present study is to clarify the relationship among the ultrasonic attenuation, low frequency dynamic mechanical properties, dielectric relaxation and Izod impact strength on the same ABS samples with various rubber content.

2. Experimental

2.1. Sample

Four ABS samples with different rubber content were prepared at Mitsubishi Chemical Co. The matrix SAN sample was prepared by radical polymerisation. Its weight average molecular weight was 1.82×10^5 and the AN content was 29 wt%. These values were determined with GPC (Waters, ALC/GPC Model 150C, Minneapolis, Minnesota) and elementary analysis (Yanaco, CHN coder, Kyoto, Japan), respectively. The rubber particles of cross-linked styrene–butadiene random copolymer SBR contains 10 wt% of styrene. At the surface of the rubber particles, the SAN molecules are grafted. Fig. 1 shows the transmission electron micrographs of the ABS samples. In these micrographs, the dark region is the rubber phase stained by osmiumtetraoxide (OsO_4). In Fig. 1, it is seen that the rubber phase has a structure similar to W/O/W emulsions [20], i.e. the rubber particles containing small SAN domains are dispersed in the SAN. The size of the rubber particles is ca. 0.2 μm on average and increases slightly with the rubber content.

The ABS samples were dried for 4 h at 180°C under a vacuum of 0.01 Torr. For ultrasonic measurements the dried ABSs were cast into rods of 30 mm diameter by compression molding at 180°C and cooled to room temperature in 30 min. The time needed for compression was ca. 10 min. Then the rods were shaped into disks with thickness of 3–20 mm on a lathe. Films of the SAN and ABSs for dielectric and mechanical measurements were also prepared by compression molding in the same manner as the samples for ultrasonic measurements.

2.2. Method

Ultrasonic measurements were performed at 1 and 10 MHz by the time of flight method [13] with PZT transducers. A fused quartz delay line was used to avoid the superposition of transmitted and reflected pulses. Each pulse contained more than 20 oscillations so that the measured velocity and attenuation corresponded to those of continuous sound wave. The contact between the sample and the transducer was achieved by putting 50/50 mixture of glycerin and isopropanol between the specimen and the transducer and the delay line. Transmission and detection of pulsed sound wave at 10 MHz were made by an apparatus

produced by Matec Instrument Co. (Model 7700, Northboro, MA, USA). Ultrasonic measurements at 1 MHz were performed with a home made pulse oscillator and detector. In the time of flight measurements, the time of flight τ_f and amplitude A of transmitted sound pulses are measured for the sample disks with different thickness d. Both of τ_f and $\log A$ are composed of two terms which are independent of the sample thickness and proportional to the thickness. For τ_f the former is due to the time of flight of the delay line and for A it is due to very small attenuation of the delay line and the reflection of the sound wave at the surface of the sample disk which contacts with the delay line. Thus from the slopes of the plots of τ_f vs. d and $\log A$ vs. d, the sound velocity V and attenuation α were determined. Temperature dependencies of V and α were measured for a sample disk of a fixed thickness by assuming that the constant terms were independent of temperature.

Dielectric measurements were made in the range of 12 Hz–200 kHz by using an RLC meter (QuadTech 1693, Maynard, MA, USA). The sample films were coated with gold by vacuum evaporation and the gold films were served as the electrode contacted tightly to the sample film. Dynamic Young's modulus and loss modulus were measured with a viscoelastic spectrometer (Iwamoto, Model VES-HF3, Kyoto, Japan) at 20 Hz. Izod impact strength was measured with an apparatus produced by Toyo Seiki (Tokyo, Japan).

3. Results and discussion

3.1. Ultrasonic behaviour

Figs. 2 and 3 show the temperature dependencies of the attenuation coefficient α of ultrasound at 1 and 10 MHz, respectively. A broad peak of α can be seen around 240 K. The attenuation coefficient increases with increasing rubber content. As is seen in Fig. 3, SAN exhibits very weak attenuation compared to the ABS samples and therefore the attenuation in ABS is attributed to the rubber phase. It is seen that the shapes of the temperature dependence curves of α at 1 and 10 MHz are different. At 1 MHz the loss curve exhibits a minimum around 270 K and above this temperature the attenuation increases with temperature. This indicates that there exist the other relaxation processes in the range above 300 K. At 10 MHz this behaviour is not seen since the relaxation region shifts to higher temperature. Fig. 4 shows the temperature dependence of the sound velocity at 10 MHz. The velocity decreases with increasing temperature due to the high attenuation peaks seen in Figs. 2 and 3. We also note that the velocity decreases with increasing rubber content. We will discuss the mechanism of the ultrasonic attenuation later.

3.2. Dynamic Young's modulus

Fig. 5 shows the storage Young's modulus E', the loss

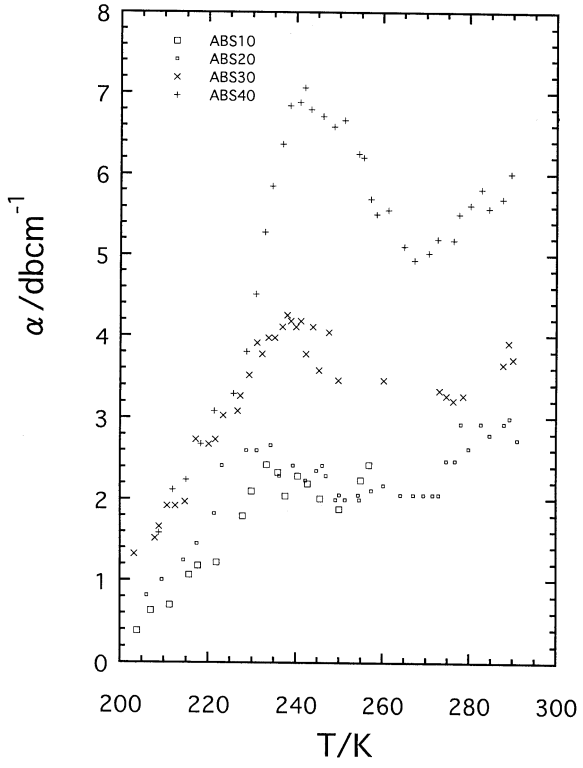

Fig. 2. Temperature dependence of the ultrasonic attenuation at 1 MHz for ABS10, ABS20, ABS30, and ABS40.

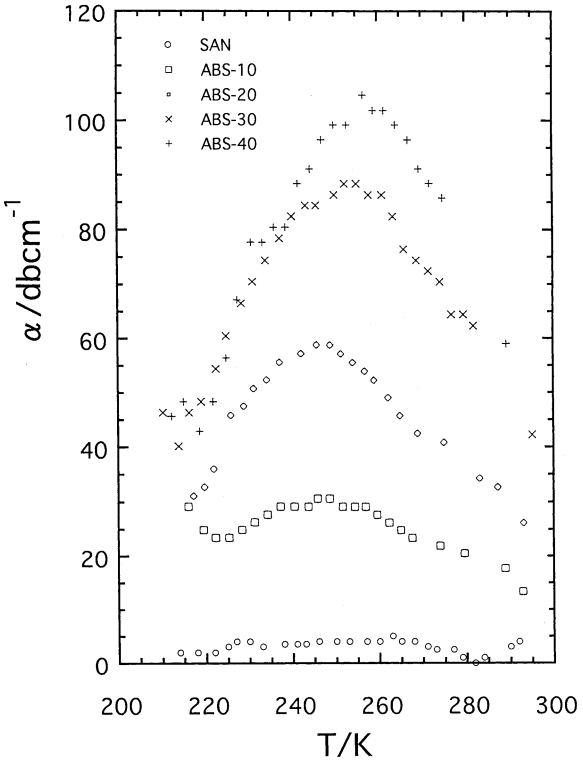

Fig. 3. Temperature dependence of the ultrasonic attenuation at 10 MHz for SAN, ABS10, ABS20, ABS30, and ABS40.

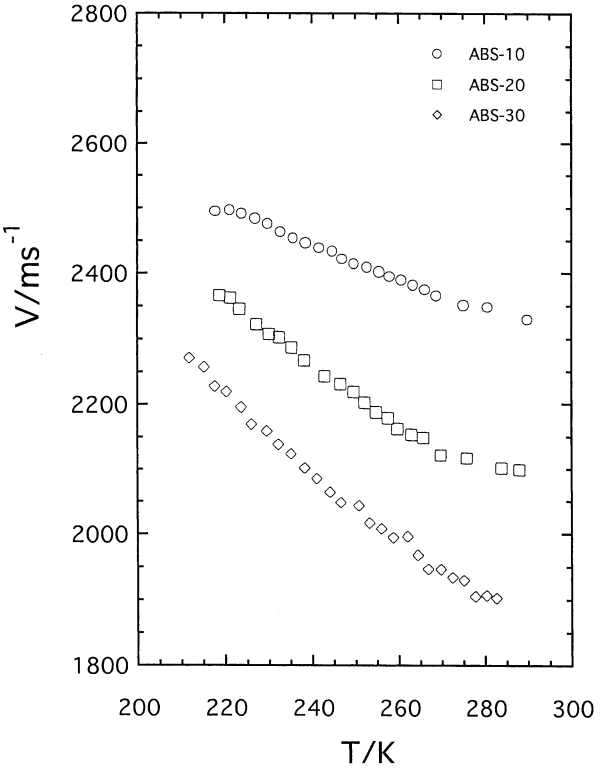

Fig. 4. Temperature dependence of the sound velocity at 10 MHz for ABS 10, ABS 20, and ABS 30.

Young's modulus E'', and tan δ at 20 Hz for ABS20 and ABS40 samples. For ABS10 and ABS30 similar behaviour was observed. Two loss peaks are seen at about +120 and −70°C. These loss peaks are designated as the α and β relaxations. The glass transition temperatures of SAN and SBR containing 10% styrene are reported to be 110 and −90°C, respectively. Obviously the high temperature peak is due to the primary α process of the matrix SAN. Aoki reported the E' and E'' of ABS with rubber content similar to the present study and assigned the β process to the primary process of the rubber particles [11]. It was found that the β peak temperature shifts to higher temperature with increasing rubber content. He explained this behaviour by considering the extra free volume created due to the difference of thermal expansion coefficient between SAN and the rubber phase [11]. In the present study the same tendency of the β peak is seen.

3.3. Dielectric relaxation

Fig. 6 shows the temperature dependence of the dielectric constant ϵ' and the loss factor ϵ'' for ABS40 at various frequencies indicated in the figure. Similar ϵ' and ϵ'' curves are observed for the other ABS samples. Fig. 7 shows the temperature dependence of ϵ'' of SAN and ABS20. The dielectric loss curve exhibits at least four loss maxima as indicated in the figure. They are designated as the α, β′, β and γ relaxations in the order of decreasing temperature.

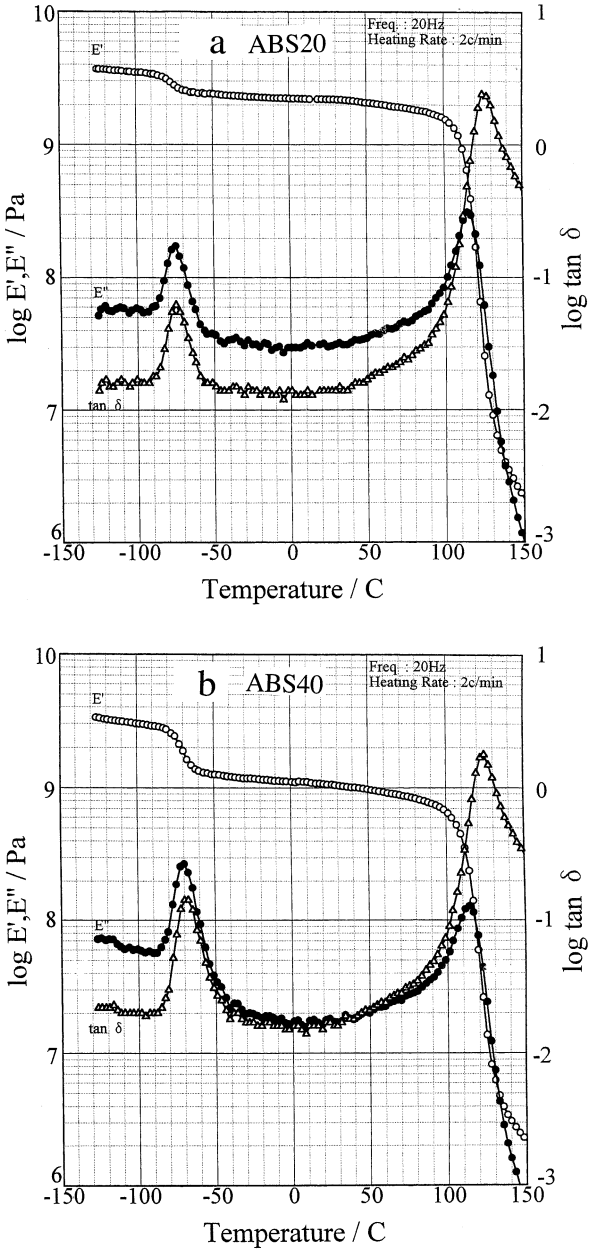

Fig. 5. Temperature dependence of the storage Young's modulus E', loss modulus E'', and tan δ at 20 Hz for (a) ABS 20 and (b) ABS 40.

The primary dielectric relaxation of SAN (32.5% acrylonitrile content) was reported to be 410 K at 1 kHz by Cook et al. [21]. Obviously the α process of the ABSs is due to the primary relaxation of the matrix SAN.

As shown in Fig. 7(a), SAN itself exhibits very broad secondary relaxation as already reported [21]. In order to see the relaxations due to the rubber phase, we subtracted the contribution of SAN to ϵ'' assuming the additivity law:

$$\Delta\epsilon'' = \epsilon''(\mathrm{ABS}) - w\epsilon''(\mathrm{SAN}) \quad (1)$$

where w denotes the weight fraction of SAN in the ABS. The validity of the additivity was discussed in our recent

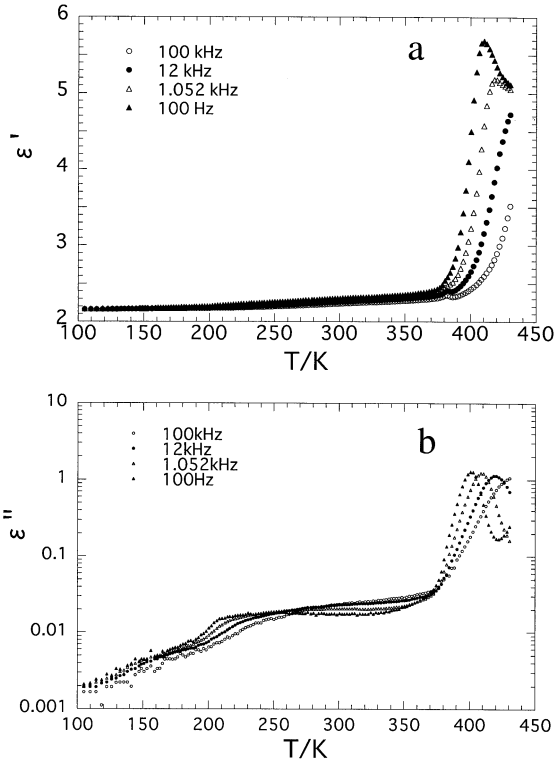

Fig. 6. Dielectric constant ϵ' and the loss factor ϵ'' of ABS40.

paper [22]. It was demonstrated that when the dielectric loss of a heterogeneous system is low, the loss could be approximately given by a weighted sum of the losses of the components. The loss of the present ABS samples exhibit the loss of the order of 0.02 and hence Eq. (1) is rationalised.

The results at 1 kHz are shown in Fig. 8. For ABS30 and ABS40, the β and β′ relaxations can be clearly distinguished. The β and β′ processes tend to merge with increasing frequency. It is seen that the intensities of these peaks increase with increasing rubber content and the shape of the $\Delta\epsilon''$ curves resembles to those of the ultrasonic attenuation.

One of the possibility of the mechanism of the β′ relaxation which was not seen in the E'' curve can be motions of low molecular weight substances contaminated in the polymerisation process. However this mechanism can be ruled out since the ABS samples purified by precipitation from toluene solution in excess amount of methanol also exhibited the β′ peak having the same intensity as the samples before purification. Therefore we assign the β′ relaxation to the motion of the butadiene and SAN chains at the surface of the rubber particles. The increase of the β′ peak with increasing rubber content is consistent with this assignment. Since the number of the segments at the surface is small compared to those of inside of the rubber particles, the β′ process was not observed in measurements of E''. However, in the dielectric measurements, this process was enhanced since the nitrile group has much higher dipole moment than that of the butadiene segments. Due to mixing of the SAN

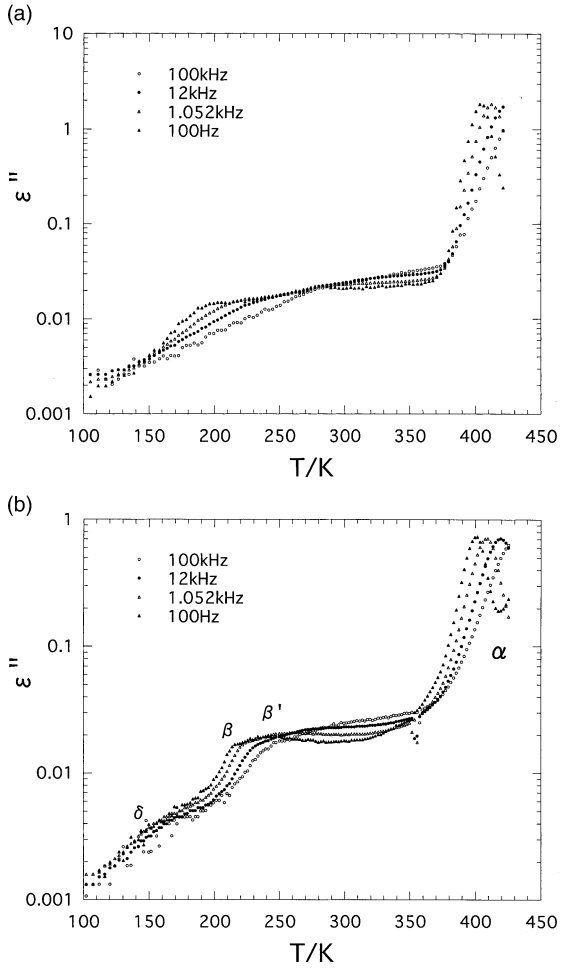

Fig. 7. Dielectric loss factor ϵ'' of (a) SAN and (b) ABS20.

and SBR the glass transition temperature of the surface area is higher than that of inside of the rubber particle and hence the β′ process locates at higher temperature than the β process. Although not shown the frequency dependence curve of ϵ'' exhibited very broad distribution of relaxation

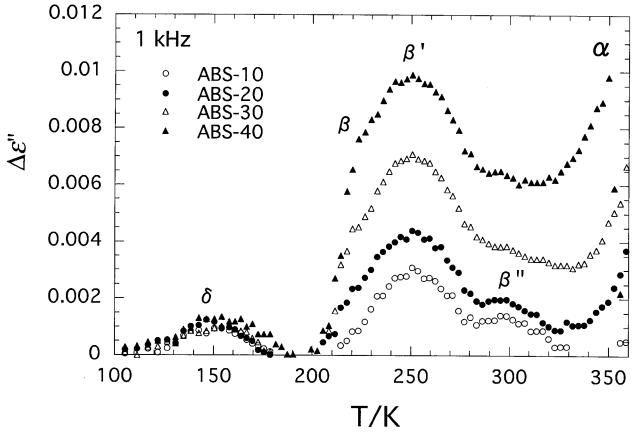

Fig. 8. The difference of the dielectric loss factor ϵ'' between ABS and SAN calculated with Eq. (1).

times reflecting the distribution of the mixing ratio of the SBR and SAN chains.

The γ process around 150 K is not seen in SAN. Therefore, this small relaxation is also attributed to the rubber particles. However in Fig. 8 we see that the intensity of this peak is almost independent of the rubber content. We speculate that the γ process is due to local mode in the glassy SBR.

Suzuki et al. studied the effect of moisture on the dielectric properties of polymers including SAN [23]. It was found that under moisture, SAN absorbs water and the dielectric loss curve exhibits a weak secondary relaxation due to motion of water molecules Therefore we dried the sample at high temperatures under a vacuum. If the ABS sample was exposed to moisture, a new relatively sharp peak appeared around at about 250 K at 1 kHz. Therefore the β, β′ and γ peaks are not due to water absorption.

Yeow and Pratt reported the dielectric relaxation of a commercial ABS [19]. The rubber content was not described. They reported that there exist seven different relaxations. In our dielectric data, such a complicated behaviour cannot be seen. Probably their ABS sample contained additives affect strongly the dielectric behaviour.

In Fig. 8, a weak loss maximum designated as the β process is seen at about 300 K. At present we do not have explanation on this process.

3.4. Mechanism of ultrasonic attenuation

In this section we consider the mechanism of the ultrasonic attenuation. The displacement ξ due to a sound wave propagating in the x direction is given by [13]

$$\xi = \xi_0 \exp[\mathrm{i}\omega(t - \Gamma^* x)] \tag{2}$$

$$\Gamma^* = \frac{1}{V} - \frac{\mathrm{i}\alpha}{\omega} \tag{3}$$

$$V^* = \frac{1}{\Gamma^*} = \sqrt{\frac{M^*}{\rho}} \tag{4}$$

where ξ_0 is the amplitude, ω the angular frequency, Γ^* the propagation constant, V^*, the complex sound velocity, ρ the density and M^* the longitudinal modulus. Here M^* is equal to $K^* + 4G^*/3$ with, the bulk modulus K^* and the shear modulus G^*. Thus, the attenuation occurs through the mechanical relaxation at high frequency.

In Fig. 9 the frequencies of measurements are plotted against the inverse of temperatures where the maxima of the ultrasonic attenuation, loss Young's modulus and dielectric loss factor are seen. We see that the mechanical and dielectric loss peaks for the β process coincide well with each other. We also note that the peaks of the ultrasonic attenuation correspond well to the β and β′ processes. Therefore, the strong ultrasonic attenuation can be assigned primarily to the segmental motions of the rubber phase. However, the attenuation cannot be totally responsible to

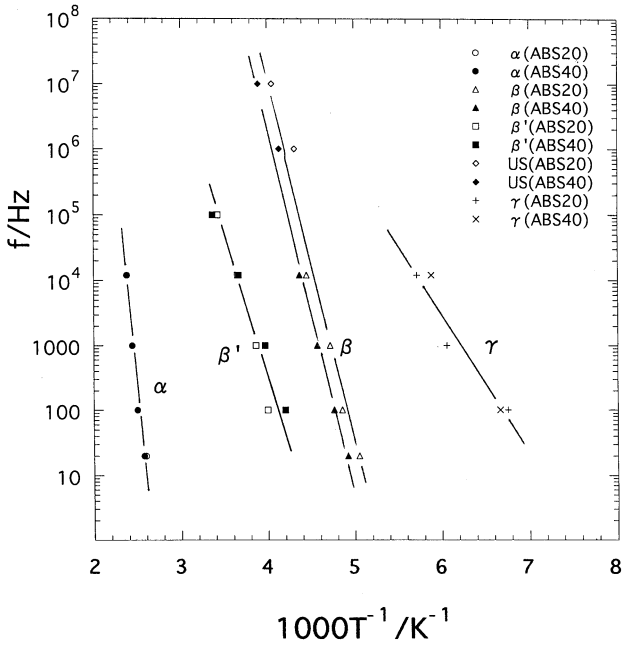

Fig. 9. Arrhenius plots of the ultrasonic attenuation, the α and β processes of the dynamic Young's moduli, and the dielectric α β, β′, and γ relaxations.

the segmental motions of the rubber phase. As seen in Fig. 2, the attenuation at 1 MHz increases with temperature around 300 K and this is due to the other mechanism than the segmental motions.

Besides the molecular relaxation processes, there are several attenuation mechanisms which are characteristic of the sound propagation, namely thermoelastic attenuation, phonon–phonon interactions, scattering, and grain heat flow [24]. The last two mechanisms are characteristic of heterogeneous systems. These mechanisms have been studied extensively for metals [19,20]. Adachi et al. studied the ultrasonic attenuation in polyethylene [14,15] and polypropylene [16]. They evaluated the contributions of these mechanisms to the attenuation and found for polyethylene that the grain heat flow between the crystalline and amorphous regions contributes much compared with the other mechanisms.

The passage of a sound wave results in oscillation of local pressure at the frequency of the sound. When the sample is compressed adiabatically temperature increases and vice versa. Thus, the sound wave causes oscillation of local temperature. In heterogeneous media composed of two microphases 1 and 2, the temperature fluctuation of domain 1 differs from that of 2. The heat flow between the phases 1 and 2 causes the increase of entropy ΔS of the system and leads to the thermoelastic losses. The decrease of the sound energy per wave length equals $T\Delta S$/(energy of sound) and the attenuation per wave length α_{ig} can be described as given in Appendix A:

$$\alpha_{ig} = \frac{\pi^2 C_{\mathrm{p2}} \beta_1^2 M_1^2 T \phi}{18 M_{\mathrm{av}} C_{\mathrm{p1}}^2} \frac{f_0 f}{f_0^2 + f^2} \tag{5}$$

$$f_0 \cong \frac{\Lambda_2}{C_{p2}L_2^2} \tag{6}$$

where suffixes 1 and 2 represent the matrix and dispersed phase, respectively, and C_p the isobaric heat capacity per unit volume, β the volume expansion coefficient, Λ the heat conductivity; and L the domain size of the grain. M and ρ have been defined for Eq. (4). We calculated f_0 and α_{ig} at $f = f_0$ for ABS20 to be 2.6 MHz and 0.013 neper/wavelength, respectively, from the data on polybutadiene, polystyrene and poly(acrylonitrile) [25]. The attenuations at 1 and 10 MHz become 0.4 and 2.5 dB/cm. This indicates that ca. 15% of the attenuation is due to the inter-grain thermoelastic effect.

Attenuation α_s due to the scattering of the sound wave was calculated by Okano [26]. He assumed a case where spherical domains (2) with radius a are dispersed in a medium (1):

$$\alpha_s = \frac{8\pi^4 a^3}{\lambda^4}\left[\frac{1}{3}\left(\frac{K_1 - K_2}{K_1}\right)^2 + \left(\frac{\rho_1 - \rho_2}{2\rho_2 + \rho_1}\right)^2\right]\phi \tag{7}$$

where λ is the wave length and K the bulk modulus. For the ABS samples, the values of α_s at 1 and 10 MHz are estimated to be of the order of 10^{-7} and 10^{-4} neper/cm, respectively, since the ratio of a/λ at 1 and 10 MHz are ca. 0.001 and 0.01, respectively. Therefore, this process does not contribute much to the present samples.

We have to check another two mechanisms of the sound attenuation. One is the sound wave–phonon interactions and the other is the classical thermoelastic process due to heat flow between the compressed and dilated parts separated by $\lambda/2$. These effects are also negligible as calculated for polyethylene [15].

3.5. Izod impact strength

Fig. 10 shows the Izod impact strength S of the ABS specimens with the rubber contents of 0–40%. It is seen that the Izod strength increases with the rubber content and becomes maximum at about 30 wt%. As discussed in Section 1, the effect of the ultrasonic attenuation on the impact strength is an interesting issue. In Fig. 10 we plotted the ultrasonic attenuation coefficient α at 300 K. It appears that there is a correlation between S and α. As described in Section 1, quick dissipation of the impact energy results in a high impact strength. The high impact strength of ABS can be attributed to at least partly to the high attenuation. The attenuation at 300 K can be ascribed to the β' and β relaxations and the inter-grain thermoelastic effects. As to the β' and β relaxations, we attributed them to the segmental motions of the rubber chains at the surface and inside of the rubber particles, respectively. It is expected that the impact stress is concentrated at the surface of the rubber particles. Thus the β' process is expected to act an important role in the sound attenuation. It is needed to test the contribution of the ultrasound absorption to the impact strength for the other polymers.

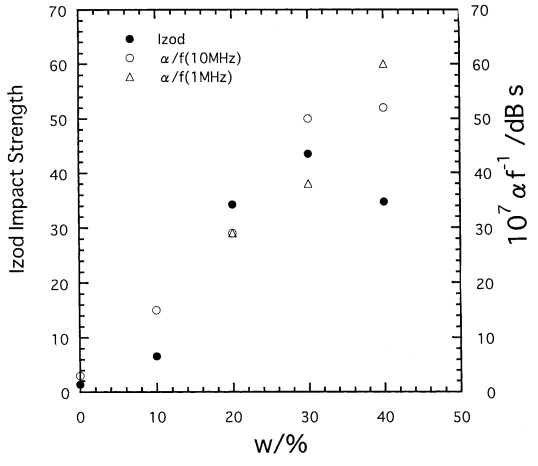

Fig. 10. The dependence of the rubber content on the Izod impact strength. The ultrasonic attenuation divided by frequency is also plotted for the sake of comparison.

4. Conclusion

The studies of ultrasonic attenuation, low frequency mechanical relaxation, dielectric relaxation, and Izod impact strength were made for ABS samples. The dielectric and dynamic mechanical data indicates that there exist four relaxation processes. They are termed α, β, β', and γ processes and can be assigned, respectively, to the primary process of the matrix SAN (α), the primary process of the rubber particles (β), the motions in the interphase (β'), and local motions of the rubber particles (γ). The ultrasonic attenuation can be ascribed to the high frequency β and β' processes. A correlation between the ultrasonic attenuation and the impact strength was recognised. Thus, the absorption of sound energy that effectively prevents formation and growth of cracks is an important factor of high impact strength of ABS. Although at the present stage, it is difficult to determine the spectrum of the Fourier components of the Izod impact, it is likely that the sound attenuation around MHz region affect most effectively the impact strength. The main mechanisms of the sound attenuation of ABS are the internal friction due to Brownian motions of the SBR chains and the inter-grain thermoelastic effect.

Appendix A

Sound attenuation due to the inter-grain thermoelastic process is derived as follows. We consider a dispersed system in which phase 2 with size a is dispersed in matrix 1. The volume fraction ϕ of the phase 2 is assumed to be much less than unity. For a homogeneous phase, the change of temperature T due to adiabatic elongation or compression

with tensile stress σ is given by

$$\frac{\partial T}{\partial \sigma} = \frac{-\beta T V}{3C_p} \tag{A1}$$

where β, V, and C_p are the volume thermal expansion coefficient, the volume, and the heat capacity per unit volume. For the longitudinal sound wave the stress σ is proportional to the longitudinal modulus $M(= K + 4G/3)$. Under adiabatic condition, temperature change ΔT due to sound wave of amplitude ξ_0 is

$$\Delta T = \frac{T\beta M}{3C_p}\xi_0 \exp(i\omega t + ikx) \tag{A2}$$

where k is the wave vector. The temperature difference ΔT_{12} between the phase 1 and 2 is given by

$$\Delta T_{12} = \frac{T}{3}\left[\frac{\beta_1 M_1}{C_{p1}} - \frac{\beta_2 M_2}{C_{p2}}\right]\xi(\omega, k) \tag{A3}$$

In the present ABS samples the modulus M of the matrix SAN is much higher than the rubber phase. On the other hand β and C_p of the phases 1 and 2 are of the same order. Thus, the second term can be neglected. Heat flow q from the matrix to the rubber phase depends on the frequency and at low frequency q is equal to $C_{p2}\Delta T_{12}\phi$ as we have assumed that the $\phi \ll 1$. Then the dissipation energy is $T\Delta S = q$ for one cycle of the sound. The attenuation per one cycle α_{ig} is given by the integral of $T\Delta S$/(sound energy) with time [24] and for the present ABS, α_{ig} is given by Eq. (5).

The relaxation frequency f_0 is given approximately by Eq. (6). For exact calculation of the time constant, it is needed to calculate the heat flow process depending on the shape of the domains. This results in the distribution of the relaxation frequency.

For the numerical calculations of Eqs. (5) and (6), we used the data given in Ref. [24], namely $\rho_1 = 1.05 \times 10^3$ kg/m^3, $\rho_2 = 1.01 \times 10^3$ kg/m^3, $\Lambda_2 = 0.20$ W/mK, $C_{p1} = 2.43 \times 10^6$ J/m^3 K, $C_{p2} = 1.91 \times 106$ J/m^3 K, $\beta_1 = 6.69 \times 10^{-4}$ K^{-1}, $M_1 \sim M_{av} = 4.45 \times 10^9$ Pa and the domain size L of the rubber phase ($= 0.2 \pm 0.1$ μm) for ABS20.

References

[1] Kulich DM, Kelley PD, Pace JE. In: Mark HF, Bikales NM, Overberger CG, Menges G, Kroschwitz JI, editors. Acrylonitrile–butadiene–styrene polymers, Encyclopedia of polymer science and engineering, vol. 1. New York: Wiley, 1985. p. 388–426.
[2] Keskkula H. Rubber-modified thermoplastics. New York: Pergamon, 2000.
[3] Kausch HH. Polymer fracture. New York: Springer, 1978.
[4] Utracki LA. Polymer alloys and blends. New York: Hanser, 1989.
[5] Matsuoka S. Relaxation phenomena in polymers. New York: Hanser, 1992. Chapter 6.
[6] Andrews EH, Reed PE. Adv Polym Sci 1978;27:1.
[7] Williams JG. Adv Polym Sci 1978;27:67.
[8] Bucknall CB. Adv Polym Sci 1978;27:121.
[9] Matsuo M. Polym Engng Sci 1969;9:205.
[10] Frazer WJ. Chem Ind 1966;94:1399.
[11] Aoki Y. Nippon Reoroji Gakkaishi 1987;15:108.
[12] Masuda T, Li L, Kitamura M, Aoki Y. Nippon Reoroji Gakkaishi 1987;15:158.
[13] Matheson AJ. Molecular acoustics. New York: Wiley, 1971.
[14] North AM, Pethrick RA, Phillips DW. Macromolecules 1977;10:992.
[15] Adachi K, Harrison G, Lamb J, North A, Pethrick RA. Polymer 1981;22:1027.
[16] Adachi K, Harrison G, Lamb J, North A, Pethrick RA. Polymer 1981;22:1081.
[17] Truell R, Elbaum C, Chick BB. Ultrasonic methods in solid state physics. New York: Academic Press, 1969.
[18] Zener C. Elasticity and anelasticity of metals. Chicago: Chicago University Press, 1948.
[19] Yeow OH, Pratt JM. Polym Int 1991;25:115.
[20] Freequard GF, Karmarker M. J Appl Polym Sci 1971;15:1649.
[21] Cook M, Williams G, Jones TT. Polymer 1975;16:835.
[22] Hayakawa T, Adachi K. Macromolecules 2000;33:6840.
[23] Suzuki T, Adachi K, Kotaka T. Polym J 1981;13:385.
[24] Zener C. Proc Phys Soc 1940;52:152.
[25] Brandrup J, Immergut EH. Polymer handbook. New York: Wiley, 1975.
[26] Okano K. 6th International Congress of Accounst (Tokyo), vol. H-61, 1968.